LIMNOLOGY
and
OCEANOGRAPHY: METHODS

ASLO

Limnol. Oceanogr.: Methods 16, 2018, 881–894

doi: 10.1002/lom3.10290

Interpretation of total phytoplankton and cyanobacteria fluorescence from cross-calibrated fluorometers, including sensitivity to turbidity and colored dissolved organic matter

Bruno Cremella [1,2]*, **Yannick Huot**,[2] **Sylvia Bonilla**[1]

[1]Phytoplankton Ecology and Physiology Group, Sección Limnología, Facultad de Ciencias, Universidad de la República, Montevideo, Uruguay

[2]Laboratory of Environmental Analysis, Université de Sherbrooke, Sherbrooke, Quebec, Canada

Abstract

In vivo pigment fluorescence methods allow simple real-time detection and quantification of freshwater algae and cyanobacteria. Available models are still limited to high-cost fluorometers, validated for single instruments or individual water bodies, preventing data comparison between multiple instruments, and thus, restricting their use in large-scale monitoring programs. Moreover, few models include corrections for optical interference (water turbidity and colored dissolved organic matter, CDOM). In this study, we developed simple models to predict phytoplankton and cyanobacterial chlorophyll *a* (Chl *a*) concentrations based on Chl *a* and C-phycocyanin in vivo fluorescence, using multiple low-cost handheld fluorometers. We aimed to: (1) fit models to mixed cyanobacterial and microalgal cultures; (2) cross-calibrate nine fluorometers of the same brand and series; (3) correct the CDOM and turbidity effects; and (4) test the algorithms' performance with natural samples. We achieved comparable results between nine instruments after the cross-calibration, allowing their simultaneous use. We obtained algorithms for total and cyanobacterial Chl *a* estimation. We developed parametric corrections to remove CDOM and turbidity interferences in the algorithms. Five sampling sites (from a lake, a stream, and an estuary) were used to test the algorithms using eight cross-calibrated fluorometers. The models showed their best performance after CDOM and turbidity corrections (total Chl *a*: R^2 = 0.99, RMSE = 7.8 μg Chl *a* L^{-1}; cyanobacterial Chl *a*: R^2 = 0.98, RMSE = 9.8 μg Chl *a* L^{-1}). In summary, our models can quantify total phytoplankton and cyanobacterial Chl *a* in real time with multiple low-cost fluorometers, allowing its implementation in large-scale monitoring programs.

Eutrophication and climate change favor toxic cyanobacterial blooms that threaten drinking and recreational water sources around the world (Chorus and Bartram 1999; Paerl and Otten 2013). Monitoring programs should include cyanobacteria biomass surveillance for the implementation of early warning alerts or for taking appropriate mitigation actions (Chorus 2012). The most widely used biomass indicators, total phytoplanktonic chlorophyll *a* concentration ([Chl *a*], μg L^{-1}) and cyanobacteria cell abundance and biovolume (Chorus and Bartram 1999) are time consuming, training intensive, and involve costly techniques (Ahn et al. 2007). Pigment fluorescence "fingerprints" has been established as an alternative approach to algae and cyanobacteria detection and quantification (Watras and Baker 1988; Lee et al. 1994). These methods are based on the distinctive fluorescence excitation and emission signals of in vivo chlorophyll *a* (Chl *a*) and phycocyanin (PC), which reflect the large evolutionary differences between cyanobacterial and algal photosynthetic antennae (Lee et al. 1995; Millie et al. 2002).

In vivo fluorescence of photosynthetic pigments is increasingly being used due to its simplicity and real-time diagnostic capacity (Ghadouani and Smith 2005; Seppälä et al. 2007; Kong et al. 2014; Zamyadi et al. 2016). Even though most of the available methods are still under evaluation, phytoplankton quantification based on in vivo fluorescence has been introduced in water management regulations (Ibelings et al. 2012), including alert system frameworks (Ahn et al. 2007; Izydorczyk et al. 2009; Koreivienė et al. 2014). However, the lack of standardization between fluorometer models and the variability in cellular pigment content and quantum yield of fluorescence, currently limit the applicability of this methodology (Zamyadi et al. 2016; Bertone et al. 2018). Despite the increasing number of publications in

*Correspondence: bruno.nicolas.cremella.palmerini@usherbrooke.ca

Additional Supporting Information may be found in the online version of this article.

this field, including multiple instrument models evaluations and set-ups (Zamyadi et al. 2012; Choo et al. 2018) most methods are instrument-specific and vary greatly among fluorometer brands and models. In particular, the excitation and emission bandwidths of fluorometers, ranging from narrow bands with higher specificity to broader wavelength ranges that reflect the overall photosynthetic absorption pigments within PSII and associated antennae, giving more sensitivity covering the variability of the phycocyanin-PSII fluorescence spectra (Seppälä et al. 2007). This leads to a gradient of different approaches for modeling the phytoplankton biomass, including a diversity in the biomass indicator used. In addition, only few available Chl *a* estimation algorithms include corrections for the biases caused by the light absorption and scattering of water constituents (Beutler et al. 2000; Ferreira et al. 2012). For logistical constraints, in the context of large-scale monitoring programs, it is necessary to develop protocols to use multiple cross-calibrated fluorometers that must return consistent and comparable results. Furthermore, given the high operational cost of large-scale programs, the use of low-cost instruments is considerably advantageous, although no standard method is available for simple, handheld fluorometers. The fluorometers on the market for in situ environmental water measurement are very diverse and address diverse needs and users: ranging from simple, handheld instruments with one or two channels, to the more complex probes with multiple excitation channels, CDOM and turbidity integrated corrections, calibrated by the manufacturer. Although the industry is continually developing more advanced and complex fluorometers, making them more reliable for research purposes or daily monitoring of individual water bodies, the accessibility of simple, handheld fluorometers made them the best choice for large geographical areas and the participation of several institutions responsible for water quality monitoring.

In natural waters, scattering and colored dissolved organic matter (CDOM) can interfere with the measurement of in vivo cell fluorescence (Brient et al. 2008; Chang et al. 2011; Ferreira et al. 2012). Due to its molecular complexity, CDOM emits fluorescence in a wide spectrum of wavelengths (Hudson et al. 2007). Scattering, often measured as "turbidity" (NTU) in monitoring programs, is caused by particles in suspension. In inland waters, its impact on the measured fluorescence can be higher than that of CDOM (Kirk 1994; Gilerson et al. 2007). Therefore, CDOM and turbidity effects must be corrected to obtain unbiased in vivo pigment fluorescence measurements. The interference of these two major factors depends on the optical configuration of each fluorometer. For example, some instruments are largely insensitive to turbidity (Zamyadi et al. 2012), while others have implemented CDOM correction using UV-excited fluorescence in their algorithms (Catherine et al. 2012). Even if the probe is susceptible to interference from turbidity and CDOM, post-measurement corrections can generally be applied (Ferreira et al. 2012). Nonetheless, there are no available methods that integrate the cross-calibration and biomass prediction model with corrections for turbidity and CDOM effects using simple handheld fluorometers yet.

In this study, we developed in vivo fluorescence correction algorithms to predict the total phytoplankton and cyanobacterial Chl *a* concentrations using multiple low-cost fluorometers of the same model to allow their implementation in large-scale monitoring programs. Four main goals were defined for this purpose: (1) to cross-calibrate and compare multiple handheld fluorometers; (2) to establish algorithms for predicting total and cyanobacterial Chl *a* concentration based on the in vivo fluorescence of Chl *a* and PC; (3) to empirically determine and correct the optical interferences of scattering and CDOM for all the sensors; and (4) to evaluate the performance of the prediction model with natural samples. While the approach was developed for a specific fluorometer brand used in a monitoring program in Uruguay, it is suitable for any other fluorometer with similar characteristics. In this work, we adapted the partitioned Chl *a* prediction models used in complex multi-excitation probes to be used with simpler, dual channel fluorometers. We challenged the use of in vivo PC fluorescence as a direct cyanobacteria biomass proxy. We sought to develop two complementary linear equations, using the fluorescence signals of the two channels, for the differentiation of eukaryote and cyanobacteria populations.

Materials and procedures

The study was carried out in four steps. First, we standardized and cross-calibrated seven handheld Aquafluor fluorometers (Turner Designs) configured with Chl *a* and PC channels (referred to as instruments I1 to I7). Second, we developed algorithms to estimate the total phytoplanktonic ($[\text{Chl}\,a]^{\text{vivo}}_{\text{tot}}$, μg Chl *a* L^{-1}) and the cyanobacterial chlorophyll *a* ($[\text{Chl}\,a]^{\text{vivo}}_{\text{cyan}}$, μg Chl *a* L^{-1}) by fitting linear models to fluorescence readings from mixed cyanobacterial and algal cultures to known Chl *a* concentrations quantified by extraction ([Chl *a*], μg Chl *a* L^{-1}). Third, we evaluated the effects of CDOM and turbidity interferences. And last, we tested the algorithms with different corrections, in natural samples from five sampling sites, using multiple cross-calibrated fluorometers.

Cultures and equipment

Four strains of cyanobacteria and three strains of microalgae (Table 1) were grown in modified BG-11 medium (Andersen et al. 2005). The experiments were conducted in Uruguay and Canada. Cultures in Uruguay were grown at 25 $\pm$ 1°C and 16 : 8 h light : dark photoperiod. Light was provided by white LED tubes (GR-T8-418LI-55C-NWRV2, Green Ray), with PAR (photosynthetically available radiation) irradiance of 60 and 80 μmol quanta m^{-2} s^{-1} for cyanobacteria and algae, respectively. Cultures in Canada were grown at

Table 1. Cyanobacteria and algae strains used in this study. UdelaR: Universidad de la República.

Strain	Origin	Classification	Cellular organization
P. agardhii MVCC11*†	Facultad de Ciencias, UdelaR	Cyanobacteria (Oscillatoriales)	Filamentous
C. raciborskii MVCC14*	Facultad de Ciencias, UdelaR	Cyanobacteria (Nostocales)	Filamentous
C. raciborskii MVCC35*	Facultad de Ciencias, UdelaR	Cyanobacteria (Nostocales)	Filamentous
C. reinhardtii B2246*	UTEX (University of Texas)	Chlorophyta	Unicellular
M. aeruginosa CPCC 299†	Canadian phycological culture collection (CPCC)	Cyanobacteria (Chroococcales)	Unicellular/ Colonial
S. obliquus CPCC5†	Canadian phycological culture collection (CPCC)	Chlorophyta	Unicellular/ Small colonies
P. tricornutum CPCC162†	Canadian phycological culture collection (CPCC)	Bacillariophyta	Unicellular

*Grown in Sección Limnología, Facultad de Ciencias, Universidad de la República, Uruguay.
†Grown in Laboratoire d'Analyses Environnementales, Université de Sherbrooke, Canada.

20 ± 1°C and 12 : 12 h light : dark photoperiod; light was provided by white fluorescent tubes (Silhouette F14T5/841/ALTO, Philips, Netherlands), with PAR irradiance of approximately 80 μmol quanta m^{-2} s^{-1}.

In vivo fluorescence was measured with handheld (0.4 kg, 18 cm of length) Aquafluor fluorometers (Turner Designs), configured with two channels corresponding to Chl *a* (part number: 8000-406; excitation 460 nm, emission ≥ 660 nm long-pass), and PC (part number: 8000-412; excitation 590 nm, central emission 673 nm with 85 nm bandpass, covering PC and Chl *a* emission bands). The fluorescence from these channels is referred to as $F_{\text{Chl }a}$ and F_{PC}, respectively. These channels predominantly gather the emission of PSII: $F_{\text{Chl }a}$ of common eukaryotic algae PSII; and F_{PC} of cyanobacterial PSII as well as the PC autofluorescence. The simultaneous use of both allows for a closer comparison between these two fractions of phytoplankton respect to more specific sensors present in other fluorometers. Fluorescence readings were done in non-fluorescent polystyrene cuvettes at room temperature (~ 20°C) and dim light. We determined that keeping the samples in the dark for 3 min was enough to reduce the impact of the non-photochemical quenching on the fluorescence readings (unpublished data), mostly in accordance with previous studies in cyanobacteria and diatoms (Ruban et al. 2004; Bailey et al. 2005; Grouneva et al. 2008).

Standardization of fluorometer outputs

Aquafluor fluorometers are designed to output calibrated values through a two-point calibration. However, we sought to work with the raw fluorescence value to develop the algorithm. To do so, we applied a standardization procedure to set up the fluorometers and then obtain the raw values.

Fluorometer outputs were standardized with a fluorescent plastic standard (Red Adjustable Solid Secondary Standards, Turner Designs, part number: 8000-952), and deionized water as the blank. The fluorescence of each sensor was linearly rescaled between 0, as the signal recorded from the blank, and 100 for the signal recorded with the solid fluorescence standard after subtracting the blank value. The fluorometer records the standard measurement internally as F_{Std} and the blank as F_{Blk} (both are reported as a percentage of the photodetector sub-saturating range), assigning to this calibration range a manual input value, Std. We arbitrarily set Std to a value of 100. The value reported by the fluorometer (F_{X}), for any sample (F_{samp}, percent of full scale), is thus equal to:

$$F_{\text{X}} = \text{Std}\left(\frac{F_{\text{samp}} - F_{\text{Blk}}}{F_{\text{Std}} - F_{\text{Blk}}}\right)$$

where the subscript X can be replaced by "Chl *a*" for the Chl *a* channel or "PC" for the phycocyanin channel. The raw values (F^*_{X}, in percentage of the photodetector sub-saturating range) with blank subtracted were then computed as:

$$F^*_{\text{X}} = F_{\text{samp}} - F_{\text{Blk}} = F_{\text{X}}\left(\frac{F_{\text{Std}} - F_{\text{Blk}}}{\text{Std}}\right) \quad (1)$$

Cross calibration of fluorometers

We performed a cross-calibration between instruments (I1 to I7) by measuring F^*_{X} from cultures of one species of algae (*Chlamydomonas reinhardtii*) and two species of cyanobacteria (*Planktothrix agardhii* and *Cylindrospermopsis raciborskii*) at three different dilutions (1, 1/10, and 1/50). Instrument I1 was used as the reference. $F^*_{\text{Chl}\,a}$ and F^*_{PC} of the culture dilutions series were measured in triplicate, giving a total of 27 readings per fluorometer. The cross-calibration coefficients (C_{Xi}) were determined by taking the median of the ratios of the F^*_{X} measured by the fluorometer i $\left(F^*_{\text{Xi},j}\right)$ to that of the fluorometer I1 $\left(F^*_{\text{X1},j}\right)$ for all samples j (each combination of species and dilution) as:

$$C_{\text{X}i} = \text{median}\left(\frac{F^*_{\text{X}i,1}}{F^*_{\text{X1},1}}, \frac{F^*_{\text{X}i,2}}{F^*_{\text{X1},2}}, \ldots \frac{F^*_{\text{X}i,n}}{F^*_{\text{X1,n}}}\right). \quad (2)$$

The cross-calibrated fluorescence values were given by:

$$F_X^{**} = \frac{F_{Xi}^{*}}{C_{Xi}}. \quad (3)$$

where F_X^{**} is the cross-calibrated fluorescence and the subscript X refers to the channel whether Chl *a* or PC. Culture subsamples were taken to measure [Chl *a*] by filtration, extraction, and spectrophotometry following ISO 10260 (ISO 1992). Linearity was assessed by measuring five dilutions of the three species with known [Chl *a*], and analyzing the slope and coefficient of linear regressions between the logarithm of the standardized fluorescence (in digital number units) and the logarithm of [Chl *a*] for each channel. The choice of logarithms was to avoid the unequal contribution of larger data points in a dilution range spanning two orders of magnitude. After the evaluation of the cross-calibration procedure using seven fluorometers, we calibrated two more instruments (I8 and I9) against I1, using cultures of *C. raciborskii* MVCC14.

Phytoplankton and cyanobacterial Chl *a* models

We sought simple models to obtain $[\mathrm{Chl}\,a]_{\mathrm{tot}}^{\mathrm{vivo}}$ and $[\mathrm{Chl}\,a]_{\mathrm{cyan}}^{\mathrm{vivo}}$. The algorithms were obtained by fitting multiple linear regressions between F_X^{**}, generated from the experiments with single and mixed cultures and [Chl *a*] measured by spectrophotometry.

We performed three experiments to simulate simple and more complex phytoplankton communities by combining (1) one cyanobacterial (*Microcystis aeruginosa*) and one algal (either *Scenedesmus obliquus* or *Phaeodactylum tricornutum*); and (2) two cyanobacterial plus two algal (*M. aeruginosa, P. agardhii, S. obliquus,* and *P. tricornutum*) cultures (Supporting Information Table S1). We quantified the Chl *a* concentration of each strain before mixing them following the extraction technique described by MacIntyre and Cullen (2005) in a calibrated Trilogy fluorometer (Turner Designs), and we measured $F_{\mathrm{Chl}\ a}$ and F_{PC} with one fluorometer (instrument I1). All data (n = 134) were used to create the data set for fitting the model.

Multiple linear regressions to estimate $[\mathrm{Chl}\,a]_{\mathrm{tot}}^{\mathrm{vivo}}$ and $[\mathrm{Chl}\,a]_{\mathrm{cyan}}^{\mathrm{vivo}}$ as a function of in vivo fluorescence were fitted according to:

$$[\mathrm{Chl}\,a]_{\mathrm{Y}}^{\mathrm{vivo}} = AF_{\mathrm{PC}}^{**} + BF_{\mathrm{Chl}\,a}^{**} \quad (4)$$

During fitting, the response variable $[\mathrm{Chl}\,a]_{Y}^{\mathrm{vivo}}$ was replaced by the known [Chl *a*]. The subscript Y can be replaced by "tot" (total phytoplanktonic Chl *a*) or "cyan" (Chl *a* of the cyanobacterial fraction of the phytoplankton) while A, and B are the regression coefficients. The response variable ([Chl *a*]) was tested for homoscedasticity using the Breusch–Pagan test (Breusch and Pagan 1979), and the residuals of the model were tested for normality using the Shapiro–Wilk test (Shapiro and Wilk 1965), to verify the fulfillment of linear regressions assumptions (Dunn and Smyth 1996). After the comparison to a model with intercept and the analysis of their variance using the Chi-squared tests for both $[\mathrm{Chl}\,a]_{\mathrm{tot}}^{\mathrm{vivo}}$ and $[\mathrm{Chl}\,a]_{\mathrm{cyan}}^{\mathrm{vivo}}$, the model without intercept was selected.

Optical interferences evaluation

To evaluate the optical interferences of turbidity and CDOM on $[\mathrm{Chl}\,a]_{\mathrm{Y}}^{\mathrm{vivo}}$ estimates, we ran two complementary experiments. First, we tested the effect of turbidity and CDOM on Chl *a* algorithms. Second, we assessed the interaction between the turbidity effects of suspended sediments and phytoplankton (represented by [Chl *a*]). To perform these experiments, we used eight cross-calibrated fluorometers (I1-I8).

To analyze the effect of turbidity, a dilution series of the kaolinite clay mineral (Droguería Paysandú, Uruguay) was made in deionized water, with turbidities of 0 (blank, actual recording 1.7 NTU), 14.8, 30.5, 62.2, 89.5, 111, 251, 497, and 755 NTU. Turbidity was measured (mean of three recordings) with a U-50 Multiparameter Water Quality Meter (Horiba, Japan). An ANOVA was carried out to examine the significance of the interactions between turbidity and the measurement of $[\mathrm{Chl}\,a]_{\mathrm{Y}}^{\mathrm{vivo}}$ with each individual fluorometer. The impact of turbidity resulting from different scatterers (kaolinite dilutions and natural water samples with different types of particles, namely sand and clay) using a single fluorometer was also examined.

The influence of CDOM was tested in a similar fashion to the turbidity gradient experiment. Commercial black tea (Lipton Yellow Label, UK) solutions were used as analogues (Seetohul et al. 2006; Dong et al. 2014) to natural freshwater CDOM (Fellman et al. 2010; Nelson and Siegel 2013). A working solution was first prepared by putting one tea bag in 450 mL of 75°C distilled water. After having reached room temperature, the solution was filtered through a fiberglass filter (MGF, Munktell, Sweden) and the absorption coefficient at 440 nm (a_{440}, m^{-1}) was measured with an Evolution 60 spectrophotometer (Thermo Fisher Scientific). The a_{440} was used as an indicator of CDOM concentration. The a_{440} (mean of three measurements) of the dilution series were: 0 m^{-1}, 6.0 m^{-1}, 12.7 m^{-1}, 19.0 m^{-1}, 25.1 m^{-1}, and 58.9 m^{-1}. We selected this range of concentrations to check for potential limits of linearity of the effect.

To check for a possible interaction between the effect of inorganic and the turbidity from the algal biomass (indicated by [Chl *a*]), combinations of a dilution series of the cyanobacterial culture *C. raciborskii* MVCC14) of 0 μg Chl *a* L^{-1}, 50 μg Chl *a* L^{-1}, and 100 μg Chl *a* L^{-1}, with three kaolinite dilutions of 0, 50, and 100 NTU were made. Turbidity was measured as previously indicated (mean of three recordings). The [Chl *a*] of the stock culture and the dilutions were quantified by filtration and extraction following ISO 10260 (ISO 1992).

For each experiment, four separate linear models were fitted for each response variable $[\text{Chl}\,a]^{\text{vivo}}_{\text{tot}}$ and $[\text{Chl}\,a]^{\text{vivo}}_{\text{cyan}}$, and their relationship with either turbidity or a_{440}, and the instrument as the categorical variable. The significance of the variables and their interaction were tested with ANOVA. For the Chl *a*–turbidity interaction experiment, the significance of the first, second, and third level interactions between the explanatory variables (measured [Chl *a*], turbidity and instrument) were tested.

Algorithm testing in natural phytoplankton samples

The algorithms for total and cyanobacterial Chl *a* estimation were tested in the field using cross-calibrated fluorometers and different sets of corrections for optical interferences. Triplicate samples collected in five water bodies in Uruguay (Canteras lake; Ramírez, Pocitos and Malvín beaches of the Río de la Plata estuary, and Carrasco stream, September 18$^{\text{th}}$, 2017, fluorescence readings, $n = 120$) were measured with eight cross-calibrated fluorometers (I2-I9). Physicochemical parameters (turbidity, temperature, pH, DO, and salinity) were obtained with a U-50 Series Multiparameter Water Quality Meter (Horiba, Japan) (mean of three measurements per site). Fresh samples were observed under an optical microscope (BX-51, Olympus, Japan) to characterize the phytoplankton composition. One-liter samples for analytical [Chl *a*] estimation were also taken from each site and transported cool and in the dark to the laboratory. [Chl *a*] was determined by spectrophotometry as described in the previous section. The fluorescence of the blank and $a_{440\text{nm}}$ was measured on water filtered through a fiberglass filter (MGF, Munktell, Sweden). As temperature can affect the in vivo pigment fluorescence, data were corrected for its effect using:

$$F^{**T}_{\text{X}} = \frac{F^{**}_{\text{X}}}{k_{T,\text{X}}(T) + c_{T,\text{X}}} \quad (5)$$

with the coefficients ($k_{T,\text{X}}$, $c_{T,\text{X}}$) from Kasinak et al. (2015) for PC (similar to values found by Hodges et al. 2018) and from Lorenzen (1966) for in vivo Chl *a*, which are consistent with the coefficients found by Watras et al. (2017). For the lab measurements described in the previous section, run at 20°C, the temperature correction factor was 1.

The performance of $[\text{Chl}\,a]^{\text{vivo}}_{\text{Y}}$ algorithms was tested using a combination of three corrections for optical interferences: (1) turbidity; (2) turbidity and a_{440}; and (3) turbidity with subtraction of blank fluorescence from the filtered water sample. The different corrections were evaluated by linear regressions between the fluorescence-predicted $[\text{Chl}\,a]^{\text{vivo}}_{\text{tot}}$ and the analytically quantified [Chl *a*], computing the root-mean-square error (RMSE).

All data analyses were performed with the R 3.4.0 software (R Core Team 2017).

Assessment

Cross-calibration of fluorometers

The PC and Chl *a* raw fluorescence ($F^{*}_{\text{X},i}$) showed linearity (PC $R^2 > 0.945$, Chl *a* $R^2 > 0.987$) with each culture dilution curve, and for all instruments (I1 to I7). The linear range went from 10 to over 1000 μg L^{-1} [Chl *a*]. These were respectively the minimum and maximum tested concentrations (Supporting Information Fig. S1), for all the species and both channels. The saturation limit was around 2000 μg Chl *a* L^{-1} for eukaryotic algae and cyanobacteria ($F^{*}_{\text{Chl}\,a}$ and F^{*}_{PC}, respectively). Significant differences were found in $F^{*}_{\text{Chl}\,a,i}$ and $F^{*}_{\text{PC},i}$ between instruments (ANOVA, $F_{6,189} = 2.22$, $p < 0.05$ for $F^{*}_{\text{PC},i}$; $F_{6,189} = 8.08$, $p < 0.05$ for $F^{*}_{\text{Chl}\,a,i}$). No particular fluorometer yielded outlier values, as shown by post-hoc Tukey's HSD tests ($p > 0.05$ for all the cases). The use of the cross-calibration product F^{**}_{X} improved the regression coefficients (R^2) between F^{**}_{PC} and extracted Chl *a* for cyanobacteria from 0.945 to 0.960, and $F^{**}_{\text{Chl}\,a}$ fluorescence and extracted Chl *a* for algae from 0.987 to 0.991, diminishing the differences between instruments. The cross-calibration coefficients ranged from 0.824 to 1.00 for the PC channel and from 0.848 to 1.01 for the Chl *a*

Table 2. Fluorometer-dependent parameters used to compute total and cyanobacterial Chl *a* using equations from Table 4.

Fluorometer	Cross-cal. factor C_{PC}	Cross-cal. factor $C_{\text{Chl}\,a}$	Turbidity effect (D_i), total Chl *a* (μg Chl *a* L^{-1} NTU^{-1})	Turbidity effect (D_i), cyano. Chl *a* (μg Chl *a* L^{-1} NTU^{-1})
I1	1.00	1.00	0.566	0.576
I2	1.00	0.848	0.317	0.316
I3	0.824	0.961	0.623	0.634
I4	0.995	1.01	0.516	0.524
I5	0.915	0.919	0.195	0.188
I6	0.828	0.853	0.212	0.203
I7	0.973	1.06	0.202	0.196
I8	2.26	1.66	0.0135	0.0102
I9	1.51	1.20	0.181	0.168

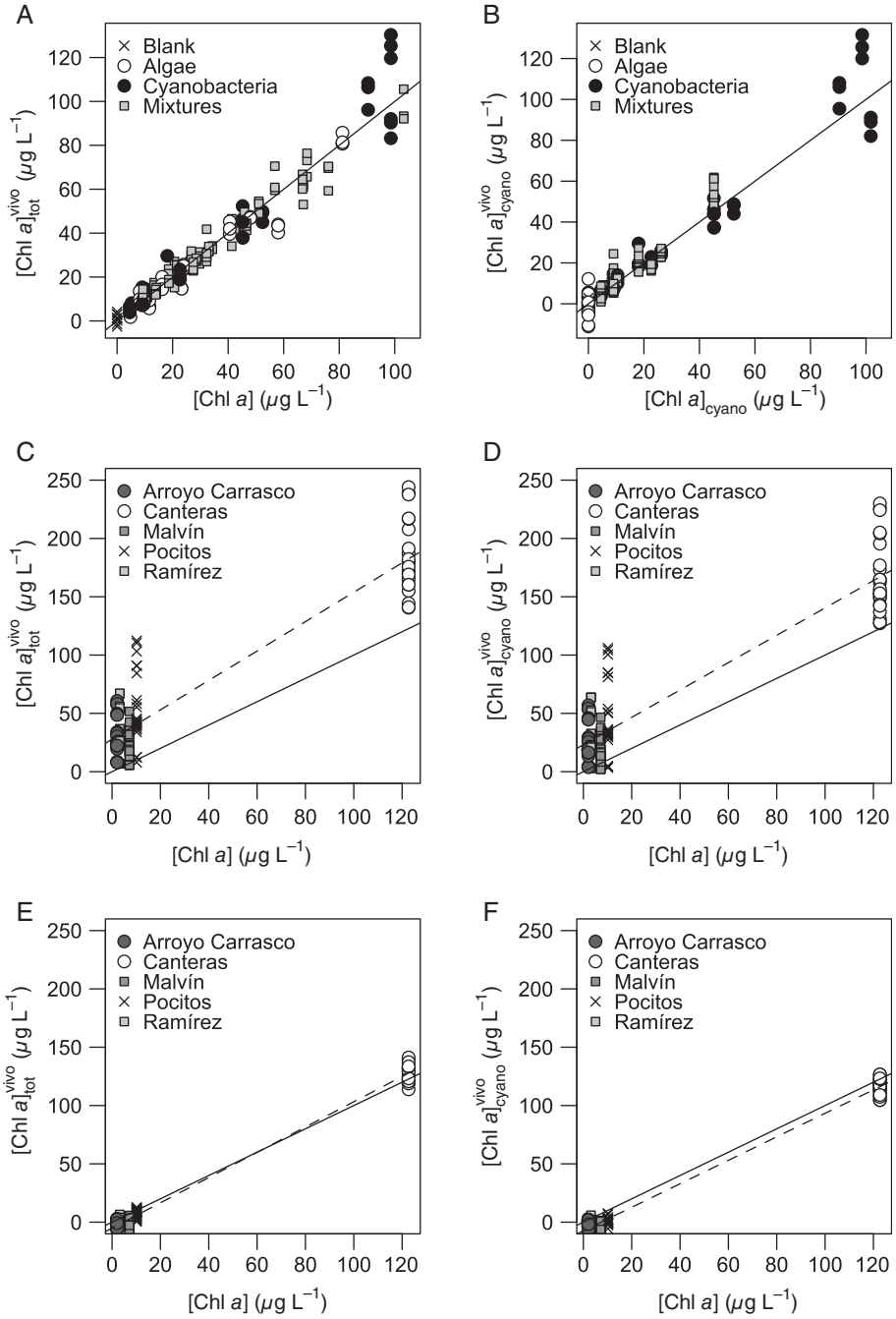

Fig. 1. Comparison between extracted total Chl *a* ([Chl *a*]) vs. Chl *a* estimated from in vivo Chl *a* and PC fluorescence using multiple regression models. Panels A and B show respectively the total ($[\text{Chl}\,a]^{\text{vivo}}_{\text{tot}}$) and cyanobacterial ($[\text{Chl}\,a]^{\text{vivo}}_{\text{cyan}}$) Chl *a* estimation from in vivo fluorescence model vs. measured [Chl *a*] in the training/culture dataset. Panels C and D show respectively $[\text{Chl}\,a]^{\text{vivo}}_{\text{tot}}$ and $[\text{Chl}\,a]^{\text{vivo}}_{\text{cyan}}$ vs. total [Chl *a*] for four field locations measured with 8 Aquafluor fluorometers using the multiple regression model without corrections. Panels E and F are the same as panels C and D but after applying the best performing corrections (*see* Table 5) for optical interferences (turbidity correction and filtrate fluorescence subtraction). For all panels, the solid line shows the 1 : 1 relation and the dashed line the linear regression. Regression models used are: $[\text{Chl}\,a]^{\text{vivo}}_{\text{tot}}$ (μg L^{-1}) = (59.8 $\pm$ 1.2)F^{**T}_{PC} + (7.96 $\pm$ 0.21)$F^{**T}_{\text{Chl}\,a}$ (R^2 = 0.986, N = 131); $[\text{Chl}\,a]^{\text{vivo}}_{\text{cyan}}$ (μg L^{-1}) = (62.4 $\pm$ 1.2) F^{**T}_{PC} - (2.57 $\pm$ 0.22) $F^{**T}_{\text{Chl}\,a}$ (R^2 = 0.957, N = 131).

channel for the seven simultaneously cross-calibrated fluorometers, belonging to the same production series (2013) (Table 2). The two extra fluorometers composed of an older (I8, 2009) and a newer (I9, 2015) production series showed a $C_{\text{PC},\,i}$ of 2.26 and 1.66, and a $C_{\text{Chl}\,a,\,i}$ of 1.51 and 1.20, respectively.

Table 3. Global parameters needed for computing the equations of the models (*see* Table 4).

Equation	Parameter	F_{PC}	$F_{Chl\ a}$
4	k_T (°C $^{-1}$)	−0.0127	−0.014
4	c_T	1.254	1.28
	Parameter	$[\text{Chl}\,a]^{vivo}_{tot}$	$[\text{Chl}\,a]^{vivo}_{cyano}$
5	F^{**}_{PC}, A (R.F.U.$_{PC}$ μg Chl a^{-1} L)	59.8±1.2	62.4±1.2
5	$F^{**}_{Chl\,a}$, B (R.F.U.$_{Chl\ a}$ μg Chl a^{-1} L)	7.96±0.21	−2.57±0.22
5	CDOM, C (μg Chl a L^{-1} m)	0.2264±0.0079	0.057±0.010

Phytoplankton and cyanobacterial Chl *a* models

Two multiple linear models were fitted to estimate the total and the cyanobacterial Chl *a* concentration, regardless of the species and pigment composition (Fig. 1). The models were fitted to data from single and mixed cultures. The response variable [Chl *a*] was homoscedastic (Breusch–Pagan test, $p > 0.05$) with [Chl *a*] < 56.5 μg L^{-1}, a condition needed for unbiased *p*-values of the linear regression parameters (Poole and O'Farrell 1971), therefore we used it as the limit range for fitting the parameters. The intercept parameter was not significant for the total Chl *a* model (intercept = 0.0 ± 0.6 μg L^{-1}, $t_{128} = -0.027$, $p = 0.98$) which was also supported by a comparison of models with- and without intercept (chi-squared test, $\chi^2_{1,\,131} = 0.008$, $p = 0.98$), and thus, the intercept was set aside. The residuals of the model were normal (Shapiro–Wilk normality test, $W = 0.981$, p-value = 0.06) up to 80 μg Chl *a* L^{-1}.

Regarding the cyanobacterial Chl *a* model, the data did not fulfill the assumptions of homogeneity of variance (Breusch–Pagan test, $p < 0.05$) at any value (tested in the full range of concentrations in increments of 1 μg Chl *a* L^{-1}). Moreover, despite the fact that residuals distribution was not normal (Shapiro–Wilk test, $W = 0.960$, $p < 0.05$), values did not depart markedly, and following the principle of parsimony, we applied the same cut-off value defined by homoscedasticity for the total Chl *a* model (= 56.5 μg L^{-1}). The parameters of the final fitted linear models for total and cyanobacterial Chl *a* (Fig. 1) were used to construct the first set of equations, to which later optical interferences corrections were added.

Table 4. Sequence of equations to compute Chl *a* concentration from in vivo Chl *a* and PC fluorescence, including the cross-calibration factors and optical interferences. Codes for factors in Table 1. NT: Turbidity in NTU.

$$F^{*}_{X} = F_{samp} - F_{Blk} = F_X \times \left(\frac{F_{Std} - F_{Blk}}{Chl_{Std}}\right) \quad (1)$$

$$C_{Xi} = \text{median}\left(\frac{F^{*}_{Xi,1}}{F^{*}_{X1,1}}, \frac{F^{*}_{Xi,2}}{F^{*}_{X1,2}}, \ldots \frac{F^{*}_{Xi,n}}{F^{*}_{X1,n}}\right) \quad (2)$$

$$F^{**}_{X} = \frac{F^{*}_{Xi}}{C_{Xi}} \quad (3)$$

$$[\text{Chl}\,a]^{vivo}_{Y} = A F^{**}_{PC} + B F^{**}_{Chl\,a} \quad (4)$$

$$F^{**T}_{X} = \frac{F^{**}_{X}}{k_{T,X}(T) + c_{T,X}} \quad (5)$$

$$[\text{Chl}\,a]^{vivo}_{Y} = A F^{**T}_{PC} + B F^{**T}_{Chl\,a} - C\,a_{440} - D_i\,\text{NT}* \quad (6)$$

Optical interferences evaluation

CDOM and turbidity interfered with the fluorescence generating a background signal which resulted in an increase in the final total and cyanobacterial Chl *a* concentration. The effect of turbidity was fluorometer-dependent as shown by ANOVA (fluorometer : turbidity interaction: $[\text{Chl}\,a]^{vivo}_{tot}$ $F_{7,\,255} = 4005.1$, $p < 0.05$: $[\text{Chl}\,a]^{vivo}_{cyan}$ $F_{7,\,255} = 3828.9$, $p < 0.05$), while the CDOM effect was the same for all instruments (fluorometer: a_{440} interaction: $[\text{Chl}\,a]^{vivo}_{tot}$ $F_{7,\,255} = 1.9$, $p > 0.05$: $[\text{Chl}\,a]^{vivo}_{cyan}$ $F_{7,\,255} = 1.7$, $p > 0.05$). The magnitude of the signal was directly proportional to CDOM absorption and turbidity, denoting a strong linear response for turbidities < 1000 NTU and $a_{440} < 50$ m^{-1}. The resulting effects of turbidity varied between 0.195–0.623 μg Chl *a* L^{-1} NTU^{-1} for total Chl *a* for I1-I7, and was 0.014 μg Chl *a* L^{-1} NTU^{-1} for I8 (old), and 0.181 μg Chl *a* L^{-1} NTU^{-1} for I9 (new). Regarding cyanobacterial Chl *a*, it varied between 0.188–0.634 μg Chl *a* L^{-1} NTU^{-1} for I1-I7, 0.010 μg Chl *a* L^{-1} NTU^{-1} for I8, and 0.168 μg Chl *a* L^{-1} NTU^{-1} for I9 (Table 2). CDOM effect was (relative to a_{440}) 0.230 μg Chl *a* L^{-1} m for total Chl *a* and 0.057 μg Chl *a* L^{-1} m for cyanobacterial Chl *a* (Table 3). For higher CDOM concentrations ($a_{440} > 50$ m^{-1}), linearity was lost, while 1000 NTU was the upper limit for turbidity quantification with the multiparameter probe. No differences were found between kaolinite and other scatterers (interaction turbidity: source $F_{1,50} = 1.21$, $p = 0.28$ and $F_{1,50} = 1.37$, $p = 0.25$ for the total and cyanobacterial Chl *a* model, respectively). The interaction between turbidity and [Chl *a*] was not significant ($[\text{Chl}\,a]^{vivo}_{tot}$ $F_{1,\,255} = 0.5$, $p > 0.05$: $[\text{Chl}\,a]^{vivo}_{cyan}$ $F_{1,\,255} = 0.7$, $p > 0.05$), as well as the triple interaction (fluorometer, turbidity, and [Chl *a*]; $[\text{Chl}\,a]^{vivo}_{tot}$ $F_{7,\,255} = 1.1$, $p > 0.05$: $[\text{Chl}\,a]^{vivo}_{cyan}$ $F_{7,\,255} = 1.0$, $p > 0.05$). This suggests that the turbidity effect can be subtracted as an independent term from the uncorrected $[\text{Chl}\,a]^{vivo}_{Y}$ to obtain a better estimation of [Chl *a*].

Due to the independent and additive nature found for the optical interferences in these particular fluorometers, both factors can be corrected by modifying Eq. 4 as:

Table 5. Regression parameters (± standard errors) and RMSE (root mean square error) of predicted Chl *a* vs. extracted Chl *a* from cultures (n = 134, training dataset) and field (n = 120) data, with the different combinations of optical interference corrections (turbidity and CDOM). Asterisks indicates significance ($p < .05$)

Model	Data set	R^2	RMSE (μg Chl *a* L^{-1})	Slope (± SE)	Intercept (± SE) (μg Chl *a* L^{-1})
Total Chl *a*	Training dataset	0.95	3.6	0.974±0.020*	0.77±0.57
	Field uncorrected	0.86	44.3	1.26±0.05*	27.8±2.6*
	Field, turbidity correction	0.95	14.6	1.09±0.02*	4.9±1.3*
	Field, turbidity, and CDOM correction	0.96	13	1.09±0.02*	3.5±1.2*
	Field, turbidity, and filtrate fluorescence subtraction	0.99	7.8	1.08±0.01*	−5.1±0.7*
Cyano. Chl *a*	Training dataset	0.92	3.9	0.967±0.025*	0.63±0.45
	Field uncorrected	0.84	37.9	1.17±0.05*	23.2±2.6*
	Field, turbidity correction	0.94	11.7	1.01±0.02*	0.4±1.3
	Field, turbidity, and CDOM correction	0.94	11.4	1.01±0.02*	0.1±1.2
	Field, turbidity, and filtrate fluorescence subtraction	0.98	9.8	1.01±0.01*	−7.4±0.7*

$$[\mathrm{Chl}\,a]_{\mathrm{Y}}^{\mathrm{vivo}} = A\,F_{\mathrm{PC}}^{**\mathrm{t}} + B\,F_{\mathrm{Chl}\,a}^{**\mathrm{t}} - C\,a_{440} - D_i\,\mathrm{NT} \quad (6)$$

where C is a correction parameter for a_{440} (CDOM measurement), and D_i is a correction parameter for turbidity (NT) for fluorometer *i*. The full set of equations integrates the normalization of fluorescence using the cross-calibration parameters, the prediction of Chl *a* with the fitted models, and the correction for optical interferences (Table 4). The equations parameters are listed in Table 2 (instrument-dependent parameters) and Table 3 (global parameters). The full set of equations along with their parameters were applied to the field data.

Algorithm testing in natural phytoplankton samples

Low [Chl *a*] (< 10 μg L^{-1}) were measured in most of the five sampling sites except for Canteras lake, where the cyanobacterium *P. agardhii* dominated the phytoplankton. In the other sites, phytoplankton was characterized by low biomass consisting of a few eukaryotes (mainly diatoms and cryptophytes). Turbidity (ranging from 36 to 156 NTU) was mainly caused by suspended sediments in Ramírez, Pocitos, and Malvín beaches, while it was due to phytoplankton in Canteras lake. Natural CDOM, ranging from < 1 m^{-1} to 14 m^{-1}, was within the a_{440} linear range of effect. Samples from Carrasco stream showed the highest a_{440} and the lowest turbidity of all the sites (Supporting Information Table S2). The regression between $[\mathrm{Chl}\,a]_{\mathrm{tot}}^{\mathrm{vivo}}$ and [Chl *a*] was significantly affected by the correction used. The RMSE decreased in the following order of corrections: (1) no correction; (2) turbidity; (3) turbidity and $a_{440\mathrm{nm}}$; and (4) turbidity and filtrate fluorescence (Table 5). While the slope was close to 1 in all cases, the fitted intercept varied greatly, was directly related to RMSE, and was mainly influenced by the effect of turbidity. A decrease in RMSE was accompanied by an increase in R^2, with a total Chl *a* R^2 of 0.86 and a cyanobacterial (using total [Chl *a*] as the independent variable) Chl *a* R^2 of 0.83 for the model without corrections, to 0.99 and 0.98, respectively, for the turbidity correction and filtrate (blank) fluorescence subtraction (Table 5).

Discussion

We developed quantitative algorithms to predict Chl *a* (total phytoplankton and cyanobacteria) with the use of simple, low-cost fluorometers. Our algorithms allow for the simultaneous use of multiple instruments (same model), which can significantly facilitate freshwater monitoring over large regions. The approach is general and could be implemented with other fluorometer brands with similar configuration.

Standardization of outputs

The fluorometers used in this study always provide outputs with the internal calibration coefficients applied. To obtain the raw ($F_{\mathrm{X},i}^{*}$) fluorescence, a back-calculation of the measurements was performed using the stored standard and blank values. The manufacturer's solid standard was used, which only works as an internal calibration standard for each instrument. Thus, a relative cross-calibration using raw fluorescence was made, with only one fluorometer calibrated with Chl *a* (I1 used later for fitting the Chl *a* prediction models). An alternative approach would be running an absolute cross-calibration using a stable fluorescent compound (like b-rhodamine, Earp et al. 2011). However, while the fluorescence solution allows the geometrical differences between

instruments to be removed, spectral differences in the emission and detection bands between brands, models, and even instruments of different production series can still lead to differences in Chl *a* calibrations. Our approach was a compromise to achieve a functional cross-calibration.

Measurements with the cross-calibrated fluorometers

The use of cross-calibration coefficients and their product, F_X^{**}, considerably improved the comparability of the data obtained with the nine tested instruments. Even though the instruments used in our study were all manufactured by the same company, minor differences in their optics affected the results, and so post-calibration corrections were a necessary step to provide comparable data. Most of the studies are restricted to single fluorometer instruments or to the comparison of different models/brands (i.e., Gregor and Marsálek 2004; Zamyadi et al. 2016; Choo et al. 2018). A few published quantitative fluorescence methods used multiple cross-calibrated instruments, although with single-channel fluorometers used in marine profiles (Briggs et al. 2011; Guinet et al. 2013; Xing et al. 2014). In our study, multiple handheld fluorometers with two channels (Chl *a* and PC) were cross-calibrated, allowing its implementation in fresh and marine aquatic environments monitoring.

Chl *a* concentration prediction algorithms

Two simple algorithms were developed to predict total and cyanobacterial Chl *a* concentrations based on in vivo fluorescence that allow multiple handheld fluorometers to provide equivalent results. Two models were fitted to data from single and mixed cultures (algae and cyanobacteria) to mimic the partitioning of Chl *a* in natural phytoplankton. By using F_X^{**}, only one instrument needs to be calibrated (fitting the Chl *a* models), as the others would use the same $[\mathrm{Chl}\,a]_Y^{\mathrm{vivo}}$ algorithms after the fluorescence cross-calibration. The algorithms are easy to implement, can be modified by the user and are adaptable to similar configuration, two-channel (Chl *a* and PC with wide emission bandpass) low-cost fluorometer, including self-assembled ones. The common approach of using in vivo Chl *a* fluorescence as a total Chl *a* proxy should be avoided in most cases in freshwater due to the common presence of cyanobacteria, and either be avoided or apply the dual channel approach.

The first available fluorescence methods that differentiated cyanobacterial from eukaryotic Chl *a* were based on tabletop spectrofluorometers (Lee et al. 1995) or in situ multi-channel probes (Beutler et al. 2002). These algorithms extended the application of the method developed by Lee et al. (1995), that consists in the use of simultaneous equations for subtracting the influence of eukaryotic algae for cyanobacterial Chl *a* quantification, using Chl *a* and PC fluorescence, and seeking for a more cost-effective, logistically flexible solution to work in the field. This permits rapid decision-taking, an important aspect for water quality monitoring programs. The extension of the models to probes with narrower PC channels will need to consider the that the greater specificity may have less interferences but may show variability in the response for the different species, as shown in the spectra evaluated by Seppälä et al. (2007). This variability will also show difficulties at the moment of integrating the channel's signal with a Chl *a* channel into a total biomass prediction model. The main advantages of our approach are: (1) the use of multiple fluorometers, a crucial aspect for its implementation on large-scale monitoring; (2) the application of parsimonious algorithms for total and cyanobacterial Chl *a* quantification; (3) the estimation of the algorithms in the 0–50 μg Chl *a* L^{-1} range, key for early cyanobacteria warnings; and (4) the integration of corrections of major optical interferences with cross-calibration and Chl *a* partition prediction.

The World Health Organization (WHO) guide for cyanobacteria monitoring in recreational waters is based on total phytoplankton Chl *a* and cyanobacterial cell abundance and biovolume (Chorus and Bartram 1999). The fluorescence-based algorithms developed here can complement these indicators by providing the cyanobacterial fraction of the phytoplanktonic Chl *a*. The use of high performance, spectral group quantifying fluorometers (i.e., AOA, Fluoroprobe and Algaetorch, bbe Moldaenke, Germany; Beutler et al. 2002, 2003) is limited in routine large-scale monitoring programs in developing countries, due to its high cost and its dependence on the manufacturer for calibration (Pires and Deltares 2010).

In our study Chl *a* was selected as the bioindicator to be estimated from fluorescence for being the universal photosynthetic pigment in phytoplankton, the best indicator tied to pigment fluorescence, widely used in monitoring programs because is a simple variable to quantify, and finally, because our algorithms can discriminate between total and cyanobacterial Chl *a*. Given the bandwidth of the channels of the Turner brand fluorometers, we can assume that they both represent well the PSII + antennae fluorescence of most common eukaryotic algae and cyanobacteria, respectively. Thus, Chl *a* is the final common indicator that reflects the concentration of PSII + antennae. The main downside of Chl *a* is its weak linearity with biovolume for some major eukaryotic groups (Catherine et al. 2012; Deblois et al. 2013; Álvarez et al. 2017). By applying the models, changes in the proportion of cyanobacteria in the total phytoplankton can be determined, which can provide an early warning alert of a future nuisance bloom. Moreover, they give the flexibility to be implemented in marine red-tide monitoring frameworks. Other commonly used biomass indicators have some limitations, thus favoring Chl *a* as the best variable to be estimated by pigment in vivo fluorescence. Phycocyanin and biovolume work well in bloom-forming cyanobacteria (Kong et al. 2014; Kasinak et al. 2015; Macário et al. 2015), but phycocyanin does not allow for a direct comparison with the eukaryotic component

without further transformations that can amplify errors and add complexity to the calculations, and biovolume is the hardest variable to determine in the lab. Cell abundance, albeit very common in cyanobacteria legislation and the literature, exhibits a poor correlation with pigment or toxin concentrations (Chorus and Bartram 1999; Kong et al. 2014; Macário et al. 2015), as Cyanobacteria cell and organism volume span more than 2 and 11 orders of magnitude, respectively (Beardall et al. 2009; Edwards et al. 2012). Based on these arguments, we chose the Chl *a* concentration as the best biomass indicator to be predicted from in vivo fluorescence.

Optical interferences

Our experimental results revealed that the turbidity effect was instrument-dependent, and very similar in magnitude between total and cyanobacterial predicted Chl *a*. Turbidity probably affected PC fluorescence by scattering the excitation light to the detector, as their excitation and emission wavelengths are very close (excitation filter < 595 nm, emission filter > 630 nm). We found that the inorganic and cellular turbidity produced the same additive effect, which allowed the subtraction of the turbidity regardless its origin. Thus, any remnant of the scattered excitation light that reaches the high sensitivity detector, will be recorded as fluorescence. It has been shown that different fluorescence probes provided different responses to turbidity depending on their specific optical configuration (Zamyadi et al. 2016). Some probes showed a positive trend in the background fluorescence with increasing turbidity (Chang et al. 2011; Yoshida et al. 2011), while others showed an opposite trend per Chl *a* slope (Beutler et al. 2002; Brient et al. 2008; Zamyadi et al. 2012). Even though most studies indicate that the effect is independent of the type of sediment (kaolinite, bentonite, or sand), Brient et al. (2008) showed that sand had a smaller effect than kaolinite did. Such different results may be explained by the diverse optical approaches to quantify turbidity. In our tests, no differences were found between the effects of the turbidity sources on fluorescence. Therefore, the use of kaolinite was enough to determine the turbidity effect. Inorganic turbidity did not show a significant interaction with phytoplankton inherent turbidity, supporting the direct correction.

CDOM contributed significantly to generating background fluorescence mostly in the Chl *a* channel, suggesting that cyanobacteria detection is less affected by CDOM than eukaryotic algae are. The response to CDOM, in contrast to the turbidity effect, was independent of the instrument. Our results show a nonlinear response between fluorescence and CDOM at $a_{440\text{nm}} > 20\ \text{m}^{-1}$. This is negligible in common natural CDOM ranges ($a_{440} < 2\ \text{m}^{-1}$), but should be taken into consideration in high CDOM sites like blackwater streams and lakes (up to $30\ \text{m}^{-1}$), and in industrial effluents (up to $100\ \text{m}^{-1}$) (Battin 1998; Gallegos 2005). A small interference effect for cyanobacterial Chl *a* was found, due to the low CDOM fluorescence in the PC channel (Fellman et al. 2010). CDOM composition may affect the fluorescence per a_{440}, and should be taken into account in high-CDOM contrasting waters (protein vs. humic CDOMs) (Fellman et al. 2010). An additional parameter, $S_{350\text{-}400\text{nm}}$ reflects CDOM molecular weight (Helms et al. 2008) and may be applied as a correction in these heavily contrasting waters. A lack of interaction between turbidity and CDOM effects was also found, allowing the use of simultaneous and independent corrections. Two alternative corrections to remove CDOM interference in the field were tested: (1) directly subtracting the fluorescence of the filtered water (blank) from the pigment fluorescence data, or (2) calculating the final Chl *a* concentration by applying an algorithm based on a CDOM concentration proxy (a_{440} or UV fluorescence). Some studies have corrected CDOM interference on pigment fluorescence in freshwaters following the two options mentioned above, directly subtracting filtered water $F_{\text{Chl } a}$ (Carlson and Shapiro 1981; Keller et al. 1990), and indirectly adding a CDOM-proportional parameter to the Chl *a* prediction algorithm (Ferreira et al. 2012). For the purposes of large-scale water monitoring programs, where access to in situ a_{440} or UV fluorescence measuring equipment is limited for institutions, the filtration method will be preferred. Nonetheless, most of the published methods do not include any correction for the fluorescence generated by natural CDOM.

In our dataset, CDOM contribution was equivalent to 30 μg L^{-1} of background Chl *a* in the urban stream (Carrasco). This is in the range of the modeled Chl *a* concentration of filtrated water in Minnesota high-CDOM forest lakes (10.5–53.4 μg Chl *a* L^{-1}, Carlson and Shapiro 1981). The effect of CDOM on beach samples (Ramírez, Pocitos, and Malvín, ~ 10 μg Chl *a* L^{-1}) was smaller and similar to the CDOM-effect Chl *a* in large fluvial ecosystems (i.e., Elbe river: ~ 10 μg L^{-1}, and Pawcatuck river: 6.87 μg L^{-1}, Beutler et al. 2000 and Keller et al. 1990, respectively). The background Chl *a* detected in our study fell within the WHO guidelines (Chorus and Bartram 1999) for cyanobacterial risk exposition in recreational waters (1 μg Chl *a* L^{-1}, 10 μg Chl *a* L^{-1}, and 50 μg Chl *a* L^{-1}, low, moderate and high risk, respectively). Consequently, the CDOM effect can be significant in the final predicted of total Chl *a* concentration, and algorithms without a CDOM correction can result in false signals of high risk of exposition to cyanobacteria, although the CDOM effect on the cyanobacterial Chl *a* is one fourth of the effect on total Chl *a* (Table 3). This interference is also particularly relevant for monitoring phytoplankton in some ecosystems like floodplain rivers as the rainfall regime could substantially and rapidly change CDOM concentration (Teixeira et al. 2011). The correction of the CDOM effect is most effective through the use of a fluorescent blank (Cullen and Davis 2002), which can be easily implemented in the field using syringe filters.

Ultimately, the corrections of CDOM and turbidity through computed parameters greatly improved the predictive performance of the algorithms. Nevertheless, instruments with an optical geometry insensitive to scattering (turbidity), or with a

turbidity sensor, and an additional CDOM fluorescence channel can significantly improve measurement reliability in field samples.

Algorithm performance in field samples

Chl *a* estimation algorithms were tested in different aquatic environments without operational constraints. As the purpose of the method was to detect cyanobacteria in the 0–50 μg Chl *a* L^{-1} range, the analysis of the RMSE was critical. The overall performance of the algorithms, first applied without optical interferences correction, showed a good R^2, although unacceptable RMSE values (44.3 μg Chl *a* L^{-1} and 37.2 μg Chl *a* L^{-1}, Table 5). However, after applying the algorithm corrections for optical interferences, the methods had significantly decreased their RMSE. The instrument-dependent correction for turbidity and the subtraction of the water filtrated fluorescence, generated a strong R^2 and the smallest RMSE (Table 5), resulting in the correction with the best predicted results. After the corrections, the performance of our algorithms significantly improved the field samples Chl *a* prediction accuracy, that fell in the range of 2–120 μg Chl *a* L^{-1} (< 10, > 90 μg L^{-1}). As bloom alerts are usually between 10 μg Chl *a* L^{-1} and 50 μg Chl *a* L^{-1} (Chorus and Bartram 1999), more data in this range are necessary to test the performance of the models for bloom predictions.

To sum up, we present new, simple quantitative models that contribute to bridging the gap between the use of in vivo pigment fluorescence for research and low-cost monitoring purposes. Nine instruments were successfully cross-calibrated with a solid standard, using different culture dilutions. For data inter-comparison, individual fluorometer coefficients should be used for post-calibration corrections. A set of equations derived from multiple linear models based on the in vivo Chl *a* and PC fluorescence accurately quantified and discriminated total and cyanobacterial Chl *a* concentration. Optical interference from CDOM and turbidity can be addressed by the addition of simple parameters to the algorithms dependent on the magnitude of each interference.

Comments and recommendations

The models could be used with any other handheld fluorometer of similar optical configuration (Chl *a* and broad PC fluorescence channels), although with different, specific parameters. This work could bring new potential to low-cost fluorometers that reported high variability in the field, which can be decreased after applying the total/cyanobacterial Chl *a* algorithms and correcting for optical interferences. We suggest that the use of in vivo PC fluorescence as a direct cyanobacteria biomass proxy and the in vivo Chl *a* fluorescence as a total Chl *a* proxy should be replaced. Instead, a set of two linear equations, using the two channels, should be used to differentiate populations, either cyanobacterial, microalgal or total Chl *a*. We also suggest that optical interferences must be corrected when possible. Most sampling teams have access to turbidimeters and filtering a small sample of water for the CDOM correction should be easily implemented. Our models show potential for application in geographically extensive water monitoring programs.

References

Ahn, C.-Y., S.-H. Joung, S.-K. Yoon, and H.-M. Oh. 2007. Alternative alert system for cyanobacterial bloom, using phycocyanin as a level determinant. J. Microbiol. **45**: 98–104.

Álvarez, E., E. Nogueira, and Á. López-Urrutia. 2017. In-vivo single-cell fluorescence and the size-scaling of phytoplankton chlorophyll content. Appl. Environ. Microbiol. **83**: e03317–e03316. doi:10.1128/AEM.03317-16

Andersen, R., J. Berges, P. Harirson, and M. Watanabe. 2005. Appendix A—Recipes for freshwater and seawater media, p. 429–528. *In* R. A. Andersenn [ed.], Algal culturing techniques. Elsevier Academic Press.

Bailey, S., N. H. Mann, C. Robinson, and D. J. Scanlan. 2005. The occurrence of rapidly reversible non-photochemical quenching of chlorophyll a fluorescence in cyanobacteria. FEBS Lett. **579**: 275–280. doi:10.1016/j.febslet.2004.11.091

Battin, T. J. 1998. Dissolved organic matter and its optical properties in a blackwater tributary of the upper Orinoco river, Venezuela. Org. Geochem. **28**: 561–569. doi:10.1016/S0146-6380(98)00028-X

Beardall, J., and others. 2009. Allometry and stoichiometry of unicellular, colonial and multicellular phytoplankton. New Phytol. **181**: 295–309. doi:10.1111/j.1469-8137.2008.02660.x

Bertone, E., M. A. Burford, and D. P. Hamilton. 2018. Fluorescence probes for real-time remote cyanobacteria monitoring: A review of challenges and opportunities. Water Res. **141**: 152–162. doi:10.1016/J.WATRES.2018.05.001

Beutler, M., K. H. Wiltshire, C. Lüring, and C. Moldaenke. 2000. Fluorometric depth-profiling of chlorophyll corrected for yellow substances. Poster Session Presented in ASLO 2000, Copenhaguen, Denmark, June 5–9.

Beutler, M., K. H. Wiltshire, B. Meyer, C. Moldaenke, C. Lüring, M. Meyerhöfer, U.-P. Hansen, and H. Dau. 2002. A fluorometric method for the differentiation of algal populations in vivo and in situ. Photosynth. Res. **72**: 39–53. doi:10.1023/A:1016026607048

Beutler, M., K. H. Wiltshire, M. Arp, J. Kruse, C. Reineke, C. Moldaenke, and U.-P. Hansen. 2003. A reduced model of the fluorescence from the cyanobacterial photosynthetic apparatus designed for the in situ detection of cyanobacteria. Biochim. Biophys. Acta **1604**: 33–46. doi:10.1016/S0005-2728(03)00022-7

Breusch, T. S., and A. R. Pagan. 1979. A simple test for heteroscedasticity and random coefficient variation. Econometrica **47**: 1287–1294. doi:10.2307/1911963

Brient, L., and others. 2008. A phycocyanin probe as a tool for monitoring cyanobacteria in freshwater bodies. J. Environ. Monit. **10**: 248–255. doi:10.1039/B714238B

Briggs, N., M. J. Perry, I. Cetinić, C. Lee, E. D'Asaro, A. M. Gray, and E. Rehm. 2011. High-resolution observations of aggregate flux during a sub-polar North Atlantic spring bloom. Deep-Sea Res. Part I Oceanogr. Res. Pap. **58**: 1031–1039. doi:10.1016/j.dsr.2011.07.007

Carlson, R. E., and J. Shapiro. 1981. Dissolved humic substances: A major source of error in fluorometric analyses involving lake waters. Limnol. Oceanogr. **26**: 785–790. doi:10.4319/lo.1981.26.4.0785

Catherine, A., N. Escoffier, A. Belhocine, A. B. Nasri, S. Hamlaoui, C. Yéprémian, C. Bernard, and M. Troussellier. 2012. On the use of the FluoroProbe®, a phytoplankton quantification method based on fluorescence excitation spectra for large-scale surveys of lakes and reservoirs. Water Res. **46**: 1771–1784. doi:10.1016/j.watres.2011.12.056

Chang, D.-W., P. Hobson, M. Burch, and T.-F. Lin. 2011. The limitation of measurement in cyanobacteria using in vivo fluoroscopy, p. 184–188. Seventh International Conference on Intelligent Sensors, Sensor Networks and Information Processing. IEEE.

Choo, F., A. Zamyadi, K. Newton, G. Newcombe, L. Bowling, R. Stuetz, and R. Henderson. 2018. Performance evaluation of in situ fluorometers for real-time cyanobacterial monitoring. H2Open **1**: 26–46. doi:10.2166/h2oj.2018.009

Chorus, I. 2012. Current approaches to cyanotoxin risk assessment, risk management and regulations in different countries. Federal Environment Agency (Umweltbundesamt).

Chorus, I., and J. Bartram. 1999, Toxic cyanobacteria in water: A guide to their public health consequences, monitoring and management. E & FN Spon.

Cullen, J. J., and R. F. Davis. 2002. Optical measurements in oceanography: When the blank makes a difference. Ocean Optics XVI Conference, Santa Fe, New Mexico.

Deblois, C. P., A. Marchand, and P. Juneau. 2013. Comparison of photoacclimation in twelve freshwater photoautotrophs (Chlorophyte, Bacillaryophyte, Cryptophyte and Cyanophyte) isolated from a natural community. PLoS One **8**: e57139. doi:10.1371/journal.pone.0057139

Dong, Y., X. Liu, L. Mei, C. Feng, C. Yan, and S. He. 2014. LED-induced fluorescence system for tea classification and quality assessment. J. Food Eng. **137**: 95–100. doi:10.1016/j.jfoodeng.2014.03.027

Dunn, P. K., and G. K. Smyth. 1996. Randomized quantile residuals. J. Comput. Graph. Stat. **5**: 236. doi:10.2307/1390802

Earp, A., and others. 2011. Review of fluorescent standards for calibration of in situ fluorometers: Recommendations applied in coastal and ocean observing programs. Opt. Express **19**: 26768. doi:10.1364/OE.19.026768, 26782

Edwards, K. F., M. K. Thomas, C. A. Klausmeier, and E. Litchman. 2012. Allometric scaling and taxonomic variation in nutrient utilization traits and maximum growth rate of phytoplankton. Limnol. Oceanogr. **57**: 554–566. doi:10.4319/lo.2012.57.2.0554

Fellman, J. B., E. Hood, and R. G. M. Spencer. 2010. Fluorescence spectroscopy opens new windows into dissolved organic matter dynamics in freshwater ecosystems: A review. Limnol. Oceanogr. **55**: 2452–2462. doi:10.4319/lo.2010.55.6.2452

Ferreira, R. D., C. C. F. Barbosa, and E. M. L. d. M. Novo. 2012. Assessment of *in vivo* fluorescence method for chlorophyll *a* estimation in optically complex waters (Curuai floodplain, Pará - Brazil). Acta Limnol. Bras. **24**: 373–386. doi:10.1590/S2179-975X2013005000011

Gallegos, C. L. 2005. Optical water quality of a blackwater river estuary: The Lower St. Johns River, Florida, USA. Estuar. Coast. Shelf Sci. **63**: 57–72. doi:10.1016/j.ecss.2004.10.010

Ghadouani, A., and R. E. H. Smith. 2005. Phytoplankton distribution in Lake Erie as assessed by a new in situ spectrofluorometric technique. J. Great Lakes Res. **31**: 154–167. doi:10.1016/S0380-1330(05)70311-7

Gilerson, A., J. Zhou, S. Hlaing, I. Ioannou, J. Schalles, B. Gross, F. Moshary, and S. Ahmed. 2007. Fluorescence component in the reflectance spectra from coastal waters. Dependence on water composition. Opt. Express **15**: 15702–15721. doi:10.1364/oe.15.015702

Gregor, J., and B. Marsálek. 2004. Freshwater phytoplankton quantification by chlorophyll a: A comparative study of in vitro, in vivo and in situ methods. Water Res. **38**: 517–522. doi:10.1016/j.watres.2003.10.033

Grouneva, I., T. Jakob, C. Wilhelm, and R. Goss. 2008. A new multicomponent NPQ mechanism in the diatom *Cyclotella meneghiniana*. Plant Cell Physiol. **49**: 1217–1225. doi:10.1093/pcp/pcn097

Guinet, C., and others. 2013. Calibration procedures and first dataset of Southern Ocean chlorophyll a profiles collected by elephant seals equipped with a newly developed CTD-fluorescence tags. Earth Syst. Sci. Data **5**: 15–29. doi:10.5194/essd-5-15-2013

Helms, J. R., A. Stubbins, J. D. Ritchie, and E. C. Minor. 2008. Absorption spectral slope ratios as indicators of molecular weight, source, and photobleaching of chromophoric dissolverd organic matter. Limnol. Oceanogr. **53**: 955–969. doi:10.4319/lo.2010.55.6.2452

Hodges, C. M., S. A. Wood, J. Puddick, C. G. McBride, and D. P. Hamilton. 2018. Sensor manufacturer, temperature, and cyanobacteria morphology affect phycocyanin fluorescence measurements. Environ. Sci. Pollut. Res. **25**: 1079–1088. doi:10.1007/s11356-017-0473-5

Hudson, N., A. Baker, and D. Reynolds. 2007. Fluorescence analysis of dissolved organic matter in natural, waste and polluted waters—a review. River Res. Appl. **23**: 631–649. doi:10.1002/rra

Ibelings, B. W., J. M. Stroom, M. Lürling, and W. E. A. Kardinaal. 2012. Netherlands: Risks of toxic cyanobacterial blooms in recreational waters and guidelines, p. 82–96. *In* I. Chorus [ed.], Current approaches to Cyanotoxin risk assessment, risk management and regulations in different countries.

ISO. 1992. ISO 10260: Water quality measurement of biochemical parameters spectrophotometric determination of chlorophyll-a concentration.

Izydorczyk, K., C. Carpentier, J. Mrówczyński, A. Wagenvoort, T. Jurczak, and M. Tarczyńska. 2009. Establishment of an alert level framework for cyanobacteria in drinking water resources by using the Algae Online Analyser for monitoring cyanobacterial chlorophyll a. Water Res. **43**: 989–996. doi:10.1016/j.watres.2008.11.048

Kasinak, J.-M. E., B. M. Holt, M. F. Chislock, and A. E. Wilson. 2015. Benchtop fluorometry of phycocyanin as a rapid approach for estimating cyanobacterial biovolume. Water Res. **13**: 455–463. doi:10.1039/c0em00163e

Keller, A. A., L. L. Beatty, L. E. Weber, and C. A. Heil. 1990. Soluble fluorescence: Effects on chlorophyll determination at different salinities. Can. J. Fish. Aquat. Sci. **47**: 1700–1709. doi:10.1139/f90-195

Kirk, J. T. O. 1994. Light and Photosynthesis in Aquatic Ecosystems, University Press, Cambridge. doi:10.1017/CBO9780511623370

Kong, Y., I. Lou, Y. Zhang, C. U. Lou, and K. M. Mok. 2014. Using an online phycocyanin fluorescence probe for rapid monitoring of cyanobacteria in Macau freshwater reservoir. Hydrobiologia **741**: 33–49. doi:10.1007/s10750-013-1759-3

Koreivienė, J., O. Anne, J. Kasperovičienė, and V. Burškytė. 2014. Cyanotoxin management and human health risk mitigation in recreational waters. Environ. Monit. Assess. **186**: 4443–4459. doi:10.1007/s10661-014-3710-0

Lee, T., M. Tsuzuki, T. Takeuchi, K. Yokoyama, and I. Karube. 1994. In-vivo fluorometric method for early detection of cyanobacterial waterblooms. J. Appl. Phycol. **6**: 489–495. doi:10.1007/BF02182403

Lee, T.-y., M. Tsuzuki, T. Takeuchi, K. Yokoyama, and I. Karube. 1995. Quantitative determination of cyanobacteria in mixed phytoplankton assemblages by an in vivo fluorimetric method. Anal. Chim. Acta **302**: 81–87. doi:10.1016/0003-2670(94)00425-L

Lorenzen, C. J. 1966. A method for the continuous measurement of in vivo chlorophyll concentration. Deep-Sea Res. Oceanogr. Abstr. **13**: 223–227. doi:10.1016/0011-7471(66)91102-8

Macário, I. P. E., B. B. Castro, M. I. S. Nunes, S. C. Antunes, C. Pizarro, C. Coelho, F. Gonçalves, and D. R. de Figueiredo. 2015. New insights towards the establishment of phycocyanin concentration thresholds considering species-specific variability of bloom-forming cyanobacteria. Hydrobiologia **757**: 155–165. doi:10.1007/s10750-015-2248-7

MacIntyre, H. L., and J. J. Cullen. 2005. Using cultures to investigate the physiological ecology of microalgae, p. 287–326. *In* R. A. Andersen [ed.], Algal culturing techniques. Elsevier Academic Press.

Millie, D. F., O. M. E. Schofield, G. J. Kirkpatrick, G. Johnsen, and T. J. Evens. 2002. Using absorbance and fluorescence spectra to discriminate microalgae. Eur. J. Phycol. **37**: 313–322. doi:10.1017/S0967026202003700

Nelson, N. B., and D. A. Siegel. 2013. The global distribution and dynamics of chromophoric dissolved organic matter. Ann. Rev. Mar. Sci. **5**: 447–476. doi:10.1146/annurev-marine-120710-100751

Paerl, H. W., and T. G. Otten. 2013. Harmful cyanobacterial blooms: Causes, consequences, and controls. Microb. Ecol. **65**: 995–1010. doi:10.1007/s00248-012-0159-y

Pires, M. D., and Deltares. 2010. Evaluation of fluorometers for the in situ monitoring of chlorophyll and/or cyanobacteria. Report prepared for DELTARES. Delft, Netherlands.

Poole, M. A., and P. N. O'Farrell. 1971. The assumptions of the linear regression model. Trans. Inst. Br. Geogr. **52**: 145–158. doi:10.2307/621706

R Core Team. 2017. R: A language and environment for statistical computing. R Foundation for Statistical Computing. Vienna, Austria.

Ruban, A., J. Lavaud, B. Rousseau, G. Guglielmi, P. Horton, and A. L. Etienne. 2004. The super-excess energy dissipation in diatom algae: Comparative analysis with higher plants. Photosynth. Res. **82**: 165–175. doi:10.1007/s11120-004-1456-1

Seetohul, L. N., M. Islam, W. T. O'Hare, and Z. Ali. 2006. Discrimination of teas based on total luminescence spectroscopy and pattern recognition. J. Sci. Food Agric. **86**: 2092–2098. doi:10.1002/jsfa.2578

Seppälä, J., P. Ylöstalo, S. Kaitala, S. Hällfors, M. Raateoja, and P. Maunula. 2007. Ship-of-opportunity based phycocyanin fluorescence monitoring of the filamentous cyanobacteria bloom dynamics in the Baltic Sea. Estuar. Coast. Shelf Sci. **73**: 489–500. doi:10.1016/j.ecss.2007.02.015

Shapiro, S. S., and M. B. Wilk. 1965. An analysis of variance test for normality (complete samples). Biometrika **52**: 591. doi:10.2307/2333709

Teixeira, M. C., J. C. R. de Azevedo, and T. A. Pagioro. 2011. Spatial and seasonal distribution of chromophoric dissolved organic matter in the Upper Paraná River floodplain environments (Brazil). Acta Limnol. Bras. **23**: 333–343. doi:10.1590/S2179-975X2012005000011

Watras, C. J., and A. L. Baker. 1988. Detection of planktonic cyanobacteria by tandem in vivo fluorometry. Hydrobiologia **169**: 77–84. doi:10.1007/BF00007935

Watras, C. J., K. A. Morrison, J. L. Rubsam, P. C. Hanson, A. J. Watras, G. D. LaLiberte, and P. Milewski. 2017. A temperature compensation method for chlorophyll and phycocyanin fluorescence sensors in freshwater. Limnol. Oceanogr.: Methods **15**: 642–652. doi:10.1002/lom3.10188

Xing, X., H. Claustre, S. Blain, F. d'Ortenzio, D. Antoine, J. Ras, and C. Guinet. 2014. Quenching correction for in vivo chlorophyll fluorescence acquired by autonomous platforms: A case study with instrumented elephant seals in the Kerguelen region (Southern Ocean). Limnol. Oceanogr. **10**: 483–495. doi:10.4319/lom.2012.10.483

Yoshida, M., T. Horiuchi, and Y. Nagasawa. 2011. In situ multi-excitation chlorophyll fluorometer for phytoplankton measurements: Technologies and applications beyond conventional fluorometers, p. 1–4. Proceedings of the OCEANS 2011 MTS/IEEE.

Zamyadi, A., N. McQuaid, S. Dorner, D. F. Bird, M. Burch, P. Baker, P. Hobson, and M. Prévost. 2012. Cyanobacterial detection using in vivo fluorescence probes: Managing interferences for improved decision-making. J. Am. Water Works Assoc. **104**: 466–480. doi:10.5942/jawwa.2012.104.0114

Zamyadi, A., F. Choo, G. Newcombe, R. Stuetz, and R. K. Henderson. 2016. A review of monitoring technologies for real-time management of cyanobacteria: Recent advances and future direction. TrAC Trends Anal. Chem. **85**: 83–96. doi:10.1016/j.trac.2016.06.023

Acknowledgments

We thank Malvina Masdeu, Andrea Somma, and Federica Hirsch for their field assistance. This work was partially financed by ANII (POS_NAC_2014_1_102517 and R1-CHA-08) and the Ministry of Environment (DINAMA), Uruguay and ELAP (2015-2016, DFATD, Canada).

Conflict of interest

None declared.

Submitted 05 June 2018
Revised 01 October 2018
Accepted 11 October 2018

Associate editor: Tammi Richardson